Decay out of superdeformed bands in the mass region $A \approx 190$ within a cluster approach

G. G. Adamian,[1,2] N. V. Antonenko,[1] R. V. Jolos,[1] Yu. V. Palchikov,[1] W. Scheid,[3] and T. M. Shneidman[1]
[1]*Joint Institute for Nuclear Research, 141980 Dubna, Russia*
[2]*Institute of Nuclear Physics, Tashkent 702132, Uzbekistan*
[3]*Institut für Theoretische Physik der Justus–Liebig–Universität, D-35392 Giessen, Germany*
(Received 19 December 2003; published 19 May 2004)

A cluster model is applied to the description of the decay out phenomenon of the yrast superdeformed states in the nuclei ^{190,192,194}Hg and ^{192,194,196}Pb. The model is based on the assumption that highly deformed cluster-type shapes are produced by a collective motion of the nuclear system in the charge asymmetry coordinate. As follows from our analysis, the sudden transition from the superdeformed minimum to the normal deformed minimum occurs because of the crossing of superdeformed band with the nearest neighboring excited normal deformed band and spreading of collective states among the compound states.

DOI: 10.1103/PhysRevC.69.054310 PACS number(s): 21.60.Ev, 21.60.Gx, 25.70.−z

I. INTRODUCTION

Over 200 superdeformed (SD) bands have been investigated in different mass regions ($A=60$, 80, 130, 150, and 190) of the nuclide chart [1]. While the rotational transitions between the SD states are easy to detect with modern Ge arrays, it is hard to localize the SD bands in excitation energy, spin, and parity and to link them to the normal deformed (ND) bands [2–6]. This is because of the remarkable feature of the SD states: the intraband $E2$ rotational transitions follow the band down with practically constant intensity and drop sharply at some spin. The whole population of the SD band goes practically to zero within two transitions. This phenomenon is referred to as the decay out of the SD band. For example, the intraband intensities show that 44% and 49% of the decay out of the band of nucleus ^{194}Hg occurs from the SD levels with spins $I^{\pi}=12^{+}$ and 10^{+}, respectively [4]. The spectrum of transitions following decay out is dominated by unresolved, overlapping γ rays, which form a statistical spectrum of the dipole character [4,7]. The one-step discrete collective γ rays to the yrast states also originate from these levels, but they carry only a small fraction of the decay out of the SD states: for example, 1.9% from each of the levels $I^{\pi}=12^{+}$ and 10^{+} of ^{194}Hg [4]. Only few discrete collective transitions between the SD and ND states have been also found in the nuclei ^{132}Nd, ^{133}Pm, ^{137}Sm, ^{139}Gd, ^{152}Dy, and ^{192,194}Pb [1,3,5,6].

The sudden disappearance of the SD bands at low spin $I \approx 6-12$ in the $A \approx 190$ region [1,4–6,8–10] and $I \approx 24-30$ in the $A \approx 150$ region [1,3] together with unobserved decay path has raised many questions concerning the mechanism of the decay out process. It has been suggested that the decay out is probably due to the mixing with ND states in the ordered or chaotic regimes [11–21]. The models of Refs. [11] attribute the suddenness of the decay out to the spin dependence of the barrier separating the SD and ND wells. The sharp decay out is explained in Ref. [17] by the increase of the tunneling probability from the SD minimum with decreasing angular momenta which occurs due to the onset of pairing. It is shown in Ref. [12] that the onset of chaos in the ND states may also imply an enhancement of the tunneling probability and provide an alternative explanation for the sudden decay out. However, some numerical calculations have been rather schematic. For example, the coupling matrix element between pure SD and ND states was used as parameter and the assumption of an exponential angular momentum dependence of this matrix element was made. The microscopical model [17] describes well the sharpness of the observed decay out in $A \approx 150$ region. However, this model has difficulties in $A \approx 190$ region that is considered in the present paper. Therefore, the question what does trigger the sudden shape change at relatively low spin still needs to be discussed.

Strong collective dipole transitions between the excited SD band and the lowest-energy SD band in ^{150}Gd, ^{152}Dy, ^{190,194}Hg, $^{196-198}$Pb and between the SD band and the ND band in ^{194}Hg and ^{194}Pb have been observed in recent experiments [3,4,6,8,10,22–24]. This indicates the possibility that the decay out is affected by the existence of a pronounced octupole deformation in the SD states. The experimentally measured properties of the excited SD bands in nuclei ^{152}Dy and ^{190,192,194}Hg have been interpreted in terms of a rotational band built on a collective octupole vibration [25]. It is worth to note that octupole vibrational states built on the fission SD isomer in ^{240}Pu have recently been reported as well [26,27]. Moreover, very large quadrupole deformations (β_2) of the SD states can lead to octupole deformations because of the appearance of both positive and negative parity single-particle states near the Fermi surface at large β_2.

Among the microscopical approaches one can distinguish the cranked shell models using a few deformation parameters and cluster models where the cluster degrees of freedom, taken properly, allow us to simplify the treatment of nuclear system in the space of collective coordinates. The coexistence of the clustering and of mean field aspects is a unique feature of nuclear many body systems. The calculations for light [28,29] and heavy nuclei [30–34] have shown that the configurations with large quadrupole and octupole deformation parameters and the low-lying collective negative parity states are strongly related to clustering. The formation and dissolution of clusters in light nuclei have been described within antisymmetrized molecular dynamics approach [29]. The α-cluster model has been used to describe the properties

of the low-lying alternating parity ND states in actinides [34]. The experimental and theoretical results provide evidence for existence of fission modes by the clustering of fissioning nuclei [35]. The energy, multipole moments, and moments of inertia of the cluster states have been found to be close to those of the SD and HD states [33].

Using the ideas mentioned above and the fact that the dynamics of a mirror asymmetric deformation can be treated as a collective motion of nucleons between the two clusters, we apply the cluster approach for the description of SD bands and for the decay out phenomenon in the present paper. Such type of collective motion creates simultaneously a deformation with even (for example, quadrupole) and odd (dipole, octupole) multipolarities. The single particle degrees of freedom are not taken explicitly into consideration. One should note that within the cluster approach we have described recently the decay out of the SD band in ^{60}Zn by discrete transitions to the ND band [36].

II. MODEL

The important modes of nuclear excitations are related to a motion in charge $\eta_Z=(Z_1-Z_2)/(Z_1+Z_2)$ and mass $\eta=(A_1-A_2)/(A_1+A_2)$ asymmetry coordinates, where Z_1 (A_1) and Z_2 (A_2) are the charge (mass) numbers of the heavy and light nuclei of the dinuclear system (DNS) [34,36,37] formed by two touching nuclei or clusters. These relevant collective variables describe the partition of nucleons between the nuclei forming the DNS. The potential energy as a function of η_Z (η) has a few minima corresponding to different clusterizations of the system. The characteristics of the states in the alpha- and ^{8}Be-, ^{12}C-cluster minima are close to those of the ND and SD bands, respectively. The wave function in η_Z can be thought as a superposition of the mononucleus configuration with $|\eta_Z|=1$ and different cluster-type configurations including the α-cluster (^{4}He-cluster) configuration with $|\eta_Z|=|\eta_Z^{\alpha}|=1-4/Z$, the ^{8}Be-cluster configuration with $|\eta_Z|=|\eta_Z^{Be}|1-8/Z$, the ^{12}C-cluster configuration with $|\eta_Z|=|\eta_Z^{C}|1-12/Z$ and other cluster ($Z=Z_1+Z_2$) configurations. The energies and moments of inertia of the symmetric three cluster configuration with two α particles on both sides of the heavy core and ^{8}Be-cluster asymmetric configuration are almost the same.

The relative contribution of each cluster component to the total wave function is determined by solving the stationary Schrödinger equation

$$H\Psi(\eta_Z,I)=E(I)\Psi(\eta_Z,I), \tag{1}$$

where the collective Hamiltonian is

$$H=-\frac{\hbar^2}{2}\frac{d}{d\eta_Z}\frac{1}{B_{\eta_Z}}\frac{d}{d\eta_Z}+U(\eta_Z,I), \tag{2}$$

with the inertia coefficient B_{η_Z} and the potential $U(\eta_Z,I)$. For cluster configurations, the potential $U(\eta_Z,I)$ in Eq. (2) is taken as a dinuclear potential energy for $|\eta_Z|<1$ [33,38],

$$U(\eta_Z,I)=V(R=R_m,\eta_Z,I)+B_1(\eta_Z)+B_2(\eta_Z)-B. \tag{3}$$

Here, the internuclear distance $R=R_m=R_1+R_2+0.5$ fm is the touching distance between the clusters. Since the N/Z-equilibrium mode is the fast one, the potential energy U is minimized with respect to the mass asymmetry η for each fixed charge asymmetry η_Z. The quantities B_1 and B_2 (which are negative) are the experimental binding energies of the clusters forming the DNS at a given mass asymmetry η and B is the binding energy of the nucleus. Due to the normalization by B, $E(I=0)=0$ for the ground state. The quantity $V(R,\eta_Z,I)$ in Eq. (3) is the nucleus-nucleus interaction potential [38],

$$V(R,\eta_Z,I)=V_C(R,\eta_Z)+V_N(R,\eta_Z)+V_{rot}(R,\eta_Z,I) \tag{4}$$

with the Coulomb V_C, the centrifugal $V_{rot}=\hbar^2I(I+1)/[2\Im(\eta_Z)]$, and the nuclear interaction V_N potentials. The potential energy $U(|\eta_Z|=1,I)$ for mononucleus is calculated as

$$U(|\eta_Z|=1,I)=U(|\eta_Z|=1,I=0)+\hbar^2I(I+1)/[2\Im(|\eta_Z|=1)]. \tag{5}$$

Calculating the potential energy for mononucleus, α, ^{7}Li, ^{8}Be, ^{11}B, ^{12}C, ^{15}N, and ^{16}O-cluster configurations by formulas (3) and (5), we interpolate the potential at discrete points by the stepwise potential.

To calculate the potential energy for $I\neq 0$, we need the moment of inertia $\Im(\eta_Z)=\Im(\eta_Z,R_m)$ [34]. As was shown in Ref. [33], the highly deformed states are well described as cluster systems and their moments of inertia are about 0.85 of the rigid-body limit of the respective cluster configuration. Following this, we assume that the moment of inertia of the cluster configurations can be expressed as

$$\Im(\eta_Z)=c_1\left(\Im_1^r+\Im_2^r+m_0\frac{A_1A_2}{A}R_m^2\right). \tag{6}$$

Here, $\Im_i^r(i=1,2)$ are rigid-body moments of inertia for the clusters in the DNS, $c_1=0.85$ for all considered nuclei, and m_0 is the nucleon mass. The rigid-body moments of inertia are calculated with deformation parameters from Ref. [39]. For $|\eta_Z|=1$, the value of the moment of inertia is not known from data because the experimental moment of inertia is a mean value between the moments of inertia of the mononucleus ($|\eta_Z|=1$) and of the contributing inertia of the cluster configurations. We assume that

$$\Im(|\eta_Z|=1)=c_2\Im^r(|\eta_Z|=1), \tag{7}$$

where $\Im^r$ is the rigid-body moment of the inertia of mononucleus and c_2 is a scaling parameter. We set $c_2=0.07$ for all nuclei under consideration in order to have a better description of the ND states with $I\geqslant 6$ which are assumed to be rotational ones.

The method of the calculation of the inertia coefficient $B_{\eta_Z}=(d\eta/d\eta_Z)^2B_\eta$ (where B_η is the mass parameter in the mass asymmetry coordinate) used for the cluster configurations is given in Ref. [40]. Since the scale of variation of η_Z is large, the η dependence of the inertia coefficient is taken

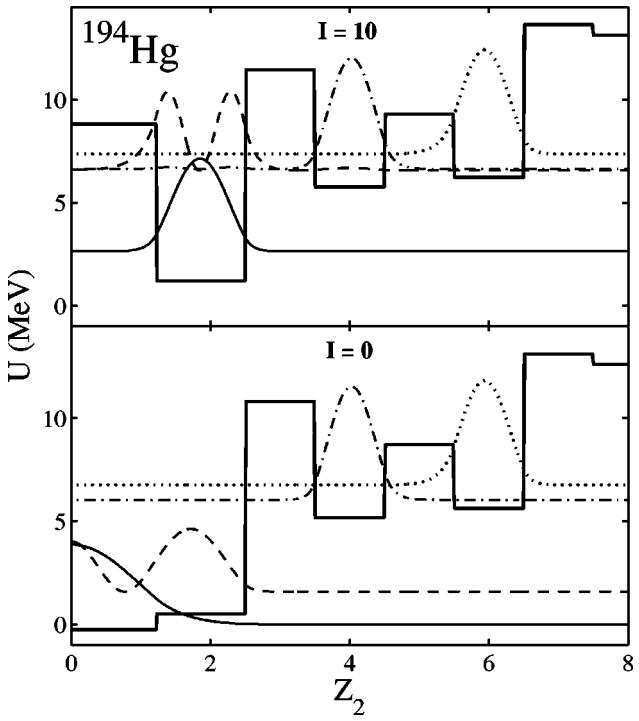

FIG. 1. Potential energy of ^{194}Hg as a function of Z_2 at spins $I=0$ and 10. Squares of the wave functions of the ground (solid curve) and first excited (dashed curve) ND bands, and ground (dash-dotted curve) and first excited SD (dotted curve) bands are shown.

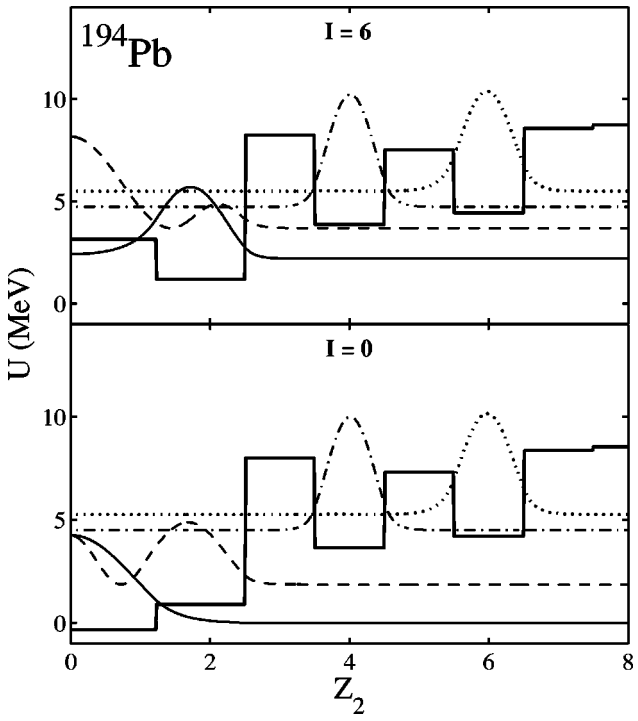

FIG. 2. The same as in Fig. 1, but for nucleus ^{194}Pb at spins $I=0$ and 6.

into consideration. Our calculations show that B_{η_Z} is a smooth function weakly dependent on the total charge number Z for $Z=80$ and 82. For all considered nuclei, we set $B_{\eta_Z}=19.2\times10^4 m_0$ fm^2 for ^{8}Be cluster configuration and $B_{\eta_Z}=12.8\times10^4 m_0$ fm^2 for ^{12}C cluster configuration. The mass parameter B_{η_Z} influences the absolute value of a zero-point vibration in the SD well. For the ND wells (mononucleus and α-cluster configuration) of all nuclei considered we set $B_{\eta_Z}=7.5\times10^4 m_0$ fm^2. With this B_{η_Z} the value of $U(|\eta_Z|=1, I=0)$ was chosen so that we obtain the correct value of the energy $E(I=0)=0$ of the ground states [34].

The electric dipole and quadrupole operators for the DNS can be obtained from the expressions [34,36,41]

$$Q_{10} = e_1^{eff} Z(\eta_Z - \eta) R_m,$$

$$Q_{20} = e\frac{Z}{2}(1 + \eta^2 - 2\eta\eta_Z)R_m^2 + Q_{20}(1) + Q_{20}(2),$$

where the charge quadrupole moments $Q_{20}(i)$ of the clusters $i=1,2$ are calculated with respect to their centers of mass. The effective charge for $E1$ transitions has been set to be equal to $e_1^{eff}=e(1+\chi)$ with $\chi=-0.7$ [42]. In the case of the quadrupole transitions we did not renormalize the charge.

III. RESULTS OF CALCULATIONS AND DISCUSSION

A. Potential energy

The important minima corresponding to the mononucleus and ^{8}Be and ^{12}C cluster configurations are shown in Figs. 1 and 2 for the nuclei ^{194}Hg and ^{194}Pb. The DNS with the α cluster has a potential energy ($I=0$) which is a little larger than the energy of the mononucleus at $|\eta_Z|=1$. At the values of $|\eta_Z|=|\eta_Z^{Li}|$ and $|\eta_Z|=|\eta_Z^{B}|$ corresponding to the ^{7}Li- and

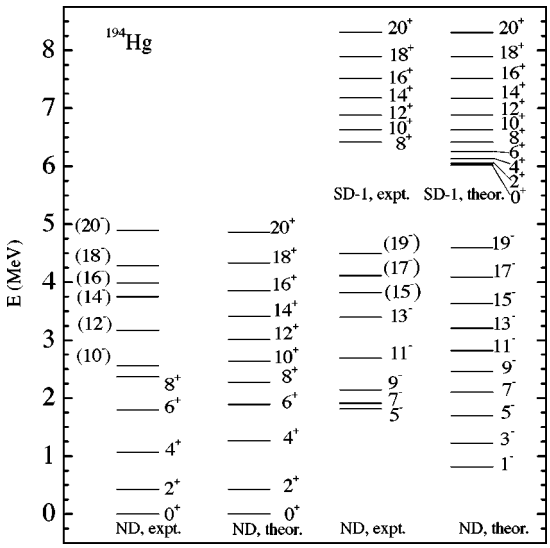

FIG. 3. Experimental (expt.) and calculated (theor.) energies of the states of the ground ND and first SD (SD-1) bands in ^{194}Hg. Experimental data are taken from Ref. [4].

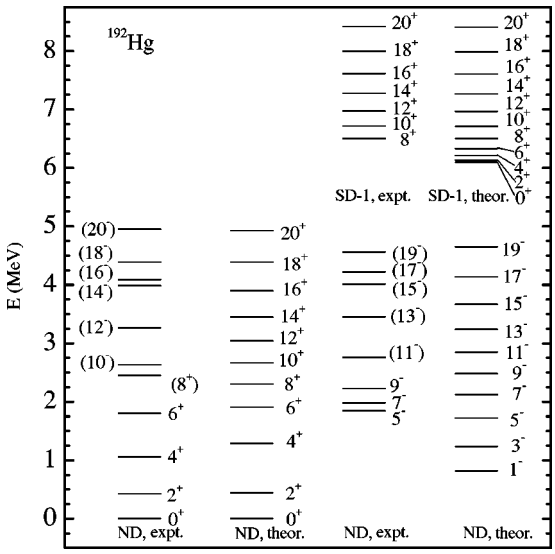

FIG. 4. The same as in Fig. 3, but for nucleus ^{192}Hg. Experimental data for the energies of transitions are taken from Ref. [9]. The experimental energies of the SD states are adjusted to have $E_{SD}^{theor}(I=8)=E_{SD}^{expt}(I=8)$.

^{11}B-cluster configurations the potential energy has maxima. The states of the ND bands have a significant contribution of the α-cluster component. The states of the ground and excited SD bands are described mainly as ^{8}Be and ^{12}C cluster configurations, respectively [41]. The SD bands lie at high energy and are isolated in a well-defined minimum from where they decay out to the ND states. The barrier separating the SD and ND minima in the ^{194}Hg nucleus smoothly decreases with spin but it remains relatively sizable for the spins corresponding to the rapid escape from the SD minimum to the ND minimum. This indicates rather pure SD states until the lowest observed member of each SD band.

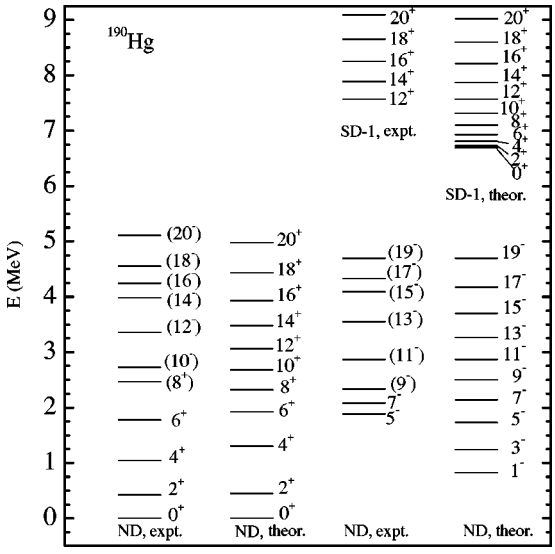

FIG. 5. The same as in Fig. 3, but for nucleus ^{190}Hg. Experimental data for the energies of transitions are taken from Ref. [8]. The experimental energies of the SD states are adjusted to have $E_{SD}^{theor}(I=12)=E_{SD}^{expt}(I=12)$.

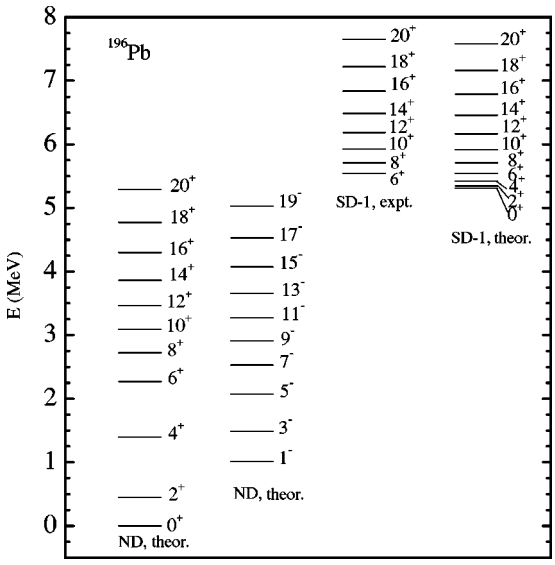

FIG. 6. The same as in Fig. 3, but for nucleus ^{196}Pb. Experimental data for the energies of transitions are taken from Ref. [10]. The experimental energies of the SD states are adjusted to have $E_{SD}^{theor}(I=6)=E_{SD}^{expt}(I=6)$.

The probability of quantum mechanical tunneling from a local minimum to an absolute minimum is a very sensitive function of the shape of the potential. The squares of the wave functions of the lowest ND and SD states taken at different spins as functions of the Z_2 (η_Z) are presented in Figs. 1 and 2. It is seen that these wave functions are well separated. Only a very small tail of the wave functions of the lowest SD state in the ND minimum supplies the small coupling of the SD state with the complex spectrum of compound states in the ND well.

Since different cluster configurations have different moments of inertia, the potential energy depends on the angular momentum of the system. This is the origin of the spin de-

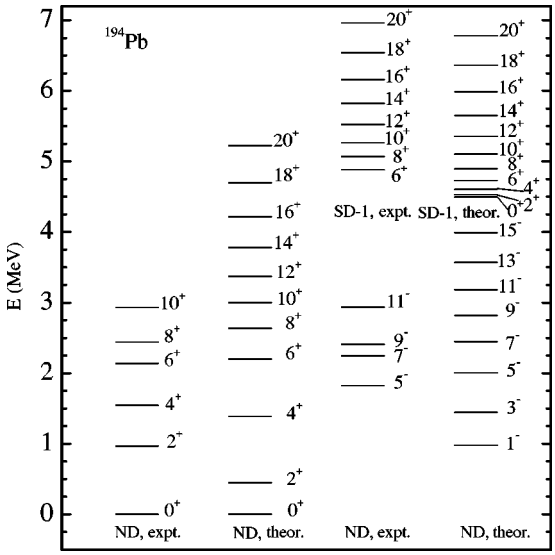

FIG. 7. The same as in Fig. 3, but for nucleus ^{194}Pb. Experimental data are taken from Ref. [6].

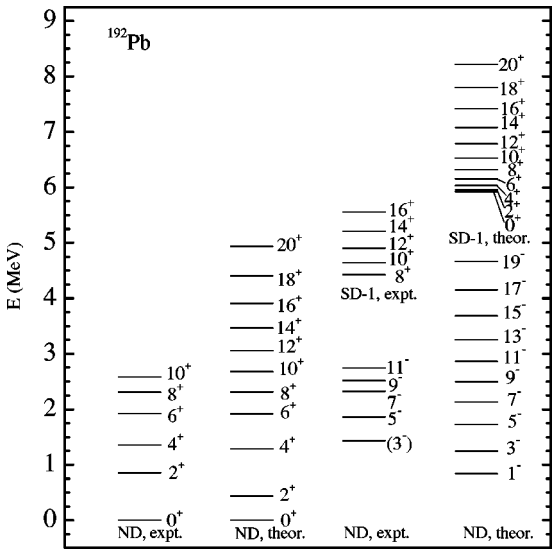

FIG. 8. The same as in Fig. 3, but for nucleus ^{192}Pb. Experimental data are taken from Ref. [5].

pendence of the mixing between the pure SD and ND states discussed in Refs. [20,21].

B. Energy spectra

Spectra of the yrast ND and SD bands for the nuclei ^{194,192,190}Hg and ^{196,194,192}Pb are shown in Figs. 3–8. One can see in the ND band that there is an appreciable shift of the negative parity states with respect to the positive parity states that is parity splitting. In the SD bands the parity splitting almost disappears. The negative parity states in the lowest SD band were not found in the experiments. As it was already mentioned in Sec. II, our investigation provides the possibility to consider the lowest SD band as a mirror symmetric cluster configuration with two α particles on both

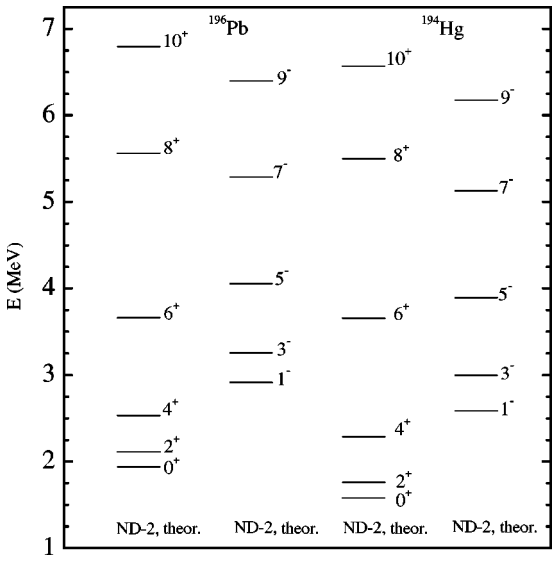

FIG. 9. Calculated energies of the states of the first excited ND band in ^{196}Pb and ^{194}Hg.

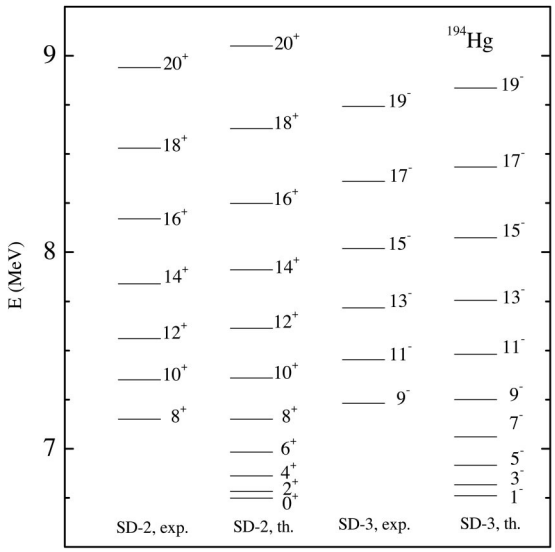

FIG. 10. Experimental (expt.) and calculated (theor.) energies of the states of the second and third SD bands (SD-2 and SD-3) in ^{194}Hg. Experimental data are taken from Ref. [4].

sides of a heavy core, e.g., $\alpha + ^{186}\mathrm{Os} + \alpha$ instead of the asymmetric configuration $^{186}\mathrm{Os} + ^{8}\mathrm{Be}$. We checked that the energies and moments of inertia of these symmetric and asymmetric cluster configurations are almost the same. Thus, it is very interesting to look in more details in the experiment whether the lowest SD states with negative parity exist or not [36].

The description of the experimental data is pretty good in the cluster approach. Since the calculated spectra of the bands are purely rotational, the deviation from the experiment seems to be caused by the influence of other degrees of freedom (other vibrations, the coupling with internal degrees of freedom). If there is doubt in the prescription of spin and parity of the measured level, its notation is given in parentheses in Figs. 3–5 for ^{194,192,190}Hg. Some of these levels are in good correspondence with the calculated ones. The yrast SD bands are well defined as rotational bands and, thus, better described than the ND bands in our approach. Further experimental and theoretical investigations of the predicted 1^- parity partners are necessary. The lack of 1^- state in the experimental rotational ND band is probably explained by the difficulties to detect this state due to the strongly enhanced $B(E1)/B(E2)$ ratio in the rotational band. If there are 3^-, 5^-, 7^-, 9^-, 11^-, 13^-,…, states, there should be 1^- state as well in the theoretical treatment. For example, the nuclei ^{218}Ra, ^{148}Ba, and ^{146}Nd have well measured alternative parity structure in the ND well but their 1^- and/or 3^- states are not experimentally observed until now [34].

The calculated excitation energies of the SD bands in ^{192,194}Hg and ^{194}Pb at zero angular momentum are in good agreement with those deduced from the experimental data [4,6,9]. In the case of ^{192}Pb (Fig. 8), we cannot reproduce the energy of the SD bandhead derived from the recent experiment [5]. The calculated SD state of ^{192}Pb with $I=10$ is 3.844 MeV above the ND yrast line and the experimental one is 2.717 MeV [5]. Decay out happens at higher I in nucleus ^{192}Pb than in nucleus ^{194}Pb because the energy of the

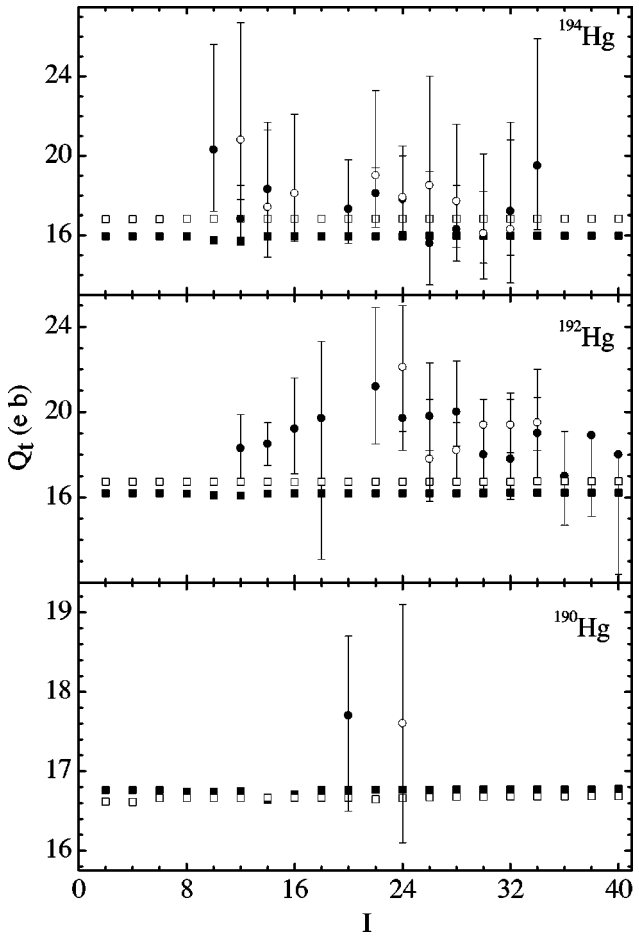

FIG. 11. The calculated (squares) and experimental (circles) [1] transition quadrupole moments Q_t in the ground (solid symbols) and first excited (open symbols) SD bands of nuclei ^{190,192,194}Hg as a function of spin I.

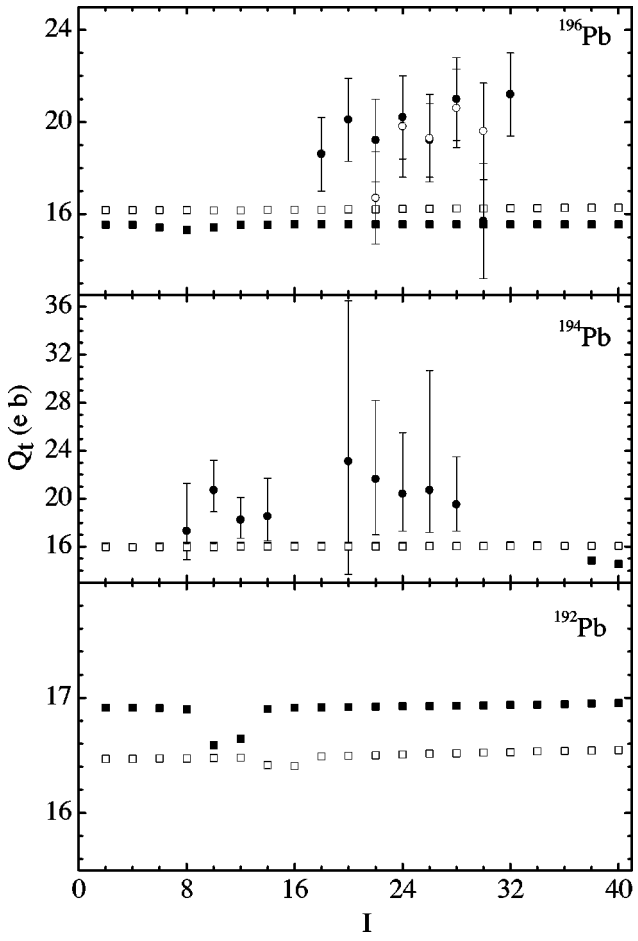

FIG. 12. The same as in Fig. 11, but for nuclei ^{192,194,196}Pb.

SD bandhead in ^{192}Pb is larger than one in ^{194}Pb. This difference between the energies of the SD bandheads in ^{192,194}Pb is mainly due to the difference between the values of nucleus-nucleus interaction in the corresponding Be-cluster configurations. Figure 9 shows the predicted energies of the states of the first excited ND bands in ^{196}Pb and ^{194}Hg. For the nucleus ^{194}Hg, the calculated levels of the first excited SD band are in agreement with the experimental levels of *SD*-2 and *SD*-3 bands (Fig. 10).

With the obtained wave functions we have calculated the reduced matrix elements of the electric dipole Q_{10} and quadrupole Q_{20} moments. In Figs. 11 and 12 the calculated transition quadrupole moments Q_t in the first and second SD bands are in satisfactory agreement with the experimental data.

C. Crossing of SD and ND bands

In Figs. 13 and 14 the energies of the ground and excited rotational ND states in the α-cluster well and of the yrast SD states in the ^{8}Be well are shown as a function of even spin for the isotopes of mercury and lead. The energies of the SD levels are lower than the energies of the nearest neighboring collective ND levels at large spins. With decreasing spin the energy interval between these states decreases and at some spin I between 6 and 14 the ND states becomes energetically lower than the SD state. In all nuclei under consideration this spin is close to the experimental spin I_{out} where the decay out happens.

Figures 15 and 16 show that the significant increase of the component

$$c^2 = \int_{|\eta_Z^{Li}|}^{1} d\eta_Z |\Psi^{SD}(\eta_Z, I)|^2 \tag{8}$$

of the SD state in the ND well takes place around the crossing point of the SD band with the nearest neighboring ND band. The increase of c^2 with decreasing spin I is mainly caused by the decreasing distance between the SD state and the nearest neighboring collective state in the ND well at the same spin.

D. Probability of decay out

In spite of relatively small ND admixture, which is the doorway state in our approach, in the SD state (for example, the maximal c^2 near the band crossing point is 2.4×10^{-2} for ^{194}Hg), the decay out can occur only through this component if the decay width Γ_{ND} of this doorway state is much larger than the decay width Γ_{SD} in the SD well.

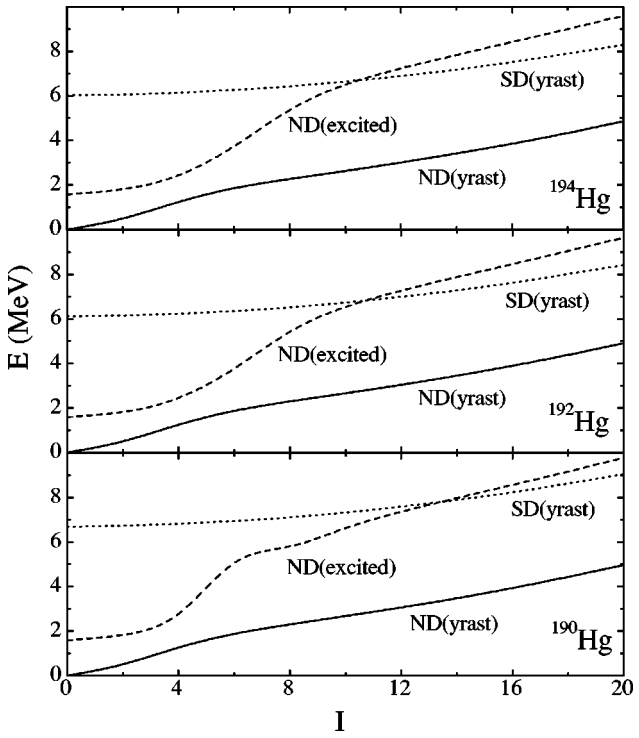

FIG. 13. The energies of ground (solid line) and first excited (dashed line) ND states with positive parity, and first SD states (dotted line) as functions of spin I for the isotopes of mercury.

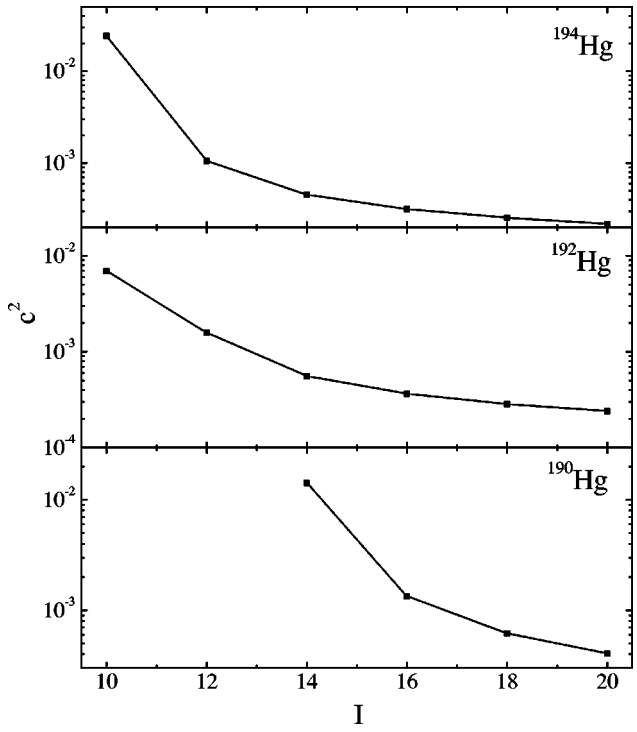

FIG. 15. The calculated ND admixture c^2 of the yrast SD states as a function of spin for the nuclei ^{190,192,194}Hg. The experimental decay out spins are I_{out}=14, 10, and 10 for ^{190,192,194}Hg, respectively [4,8,9].

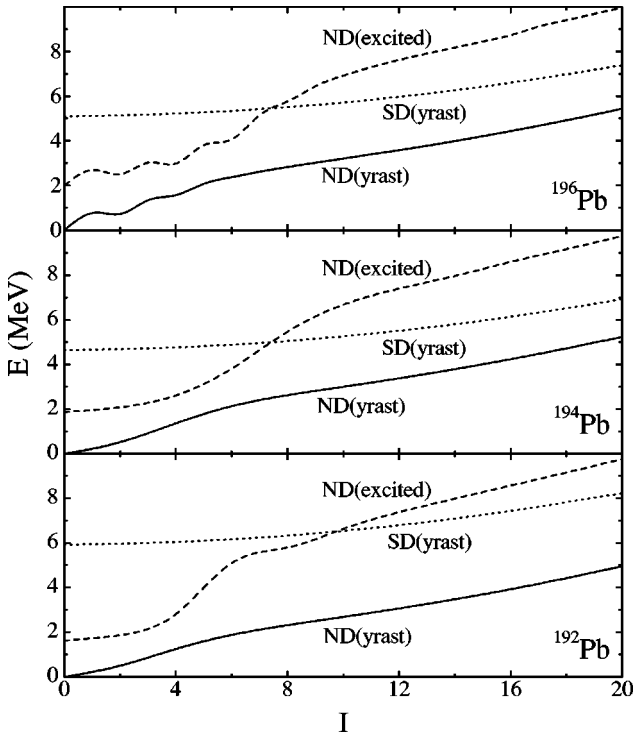

FIG. 14. The same as in Fig. 13, but for the isotopes of lead.

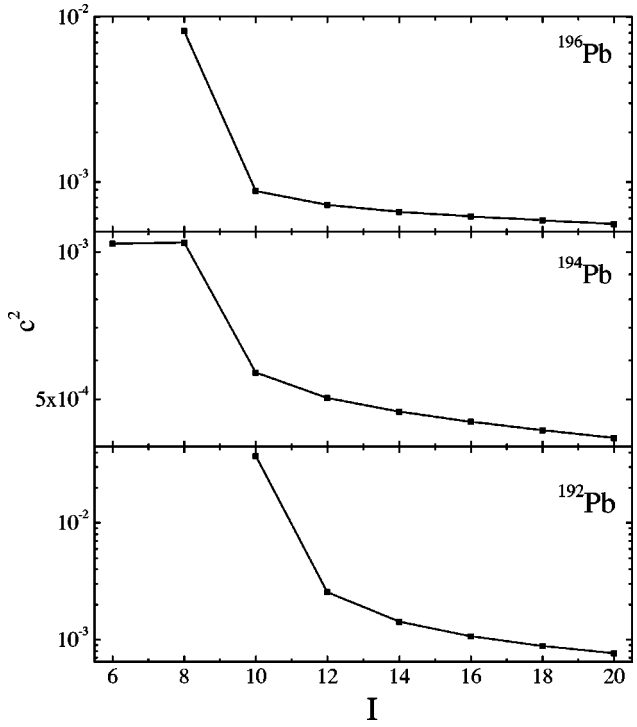

FIG. 16. The same as in Fig. 15, but for the nuclei ^{192,194,196}Pb. The experimental decay out spins are I_{out}=10, 6, and 8 for ^{192,194,196}Pb, respectively [6,5,10].

TABLE I. The calculated (Theor.) and experimental (Expt.) branching ratios of the decay intensities of the one-step discrete $E1$ and $E2$ transitions. The calculations are performed near the band crossings. Experimental data are taken from Ref. [4].

	^{194}Hg		^{190}Hg		^{194}Pb	
Ratio	Expt.	Theor.	Expt.	Theor.	Expt.	Theor.
$T(E1;6^+_{SD}\to 7^-_{ND})/T(E2;6^+_{SD}\to 4^+_{SD})$						0.12
$T(E1;6^+_{SD}\to 5^-_{ND})/T(E2;6^+_{SD}\to 4^+_{SD})$						0.11
$T(E1;8^+_{SD}\to 9^-_{ND})/T(E2;8^+_{SD}\to 6^+_{SD})$						0.028
$T(E1;8^+_{SD}\to 7^-_{ND})/T(E2;8^+_{SD}\to 6^+_{SD})$						0.031
$T(E1;10^+_{SD}\to 11^-_{ND})/T(E2;10^+_{SD}\to 8^+_{SD})$	0.13	0.034				0.007
$T(E1;10^+_{SD}\to 9^-_{ND})/T(E2;10^+_{SD}\to 8^+_{SD})$	0.73	0.037				0.009
$T(E1;12^+_{SD}\to 13^-_{ND})/T(E2;12^+_{SD}\to 10^+_{SD})$	0.020	0.022				
$T(E1;12^+_{SD}\to 11^-_{ND})/T(E2;12^+_{SD}\to 10^+_{SD})$	0.022	0.019				
$T(E1;14^+_{SD}\to 15^-_{ND})/T(E2;14^+_{SD}\to 12^+_{SD})$		0.006		0.007		
$T(E1;14^+_{SD}\to 13^-_{ND})/T(E2;14^+_{SD}\to 12^+_{SD})$		0.007		0.008		
$T(E1;16^+_{SD}\to 17^-_{ND})/T(E2;16^+_{SD}\to 14^+_{SD})$				0.001		
$T(E1;16^+_{SD}\to 15^-_{ND})/T(E2;16^+_{SD}\to 14^+_{SD})$				0.001		
$T(E1;18^+_{SD}\to 19^-_{ND})/T(E2;18^+_{SD}\to 16^+_{ND})$				0.0004		
$T(E1;18^+_{SD}\to 17^-_{ND})/T(E2;18^+_{SD}\to 16^+_{SD})$				0.0006		

1. One-step transitions

The calculated transition strengths for the one-step branches in nuclei ^{194}Hg and ^{194}Pb are about 10^{-8} W.u. for the $E1$ multipolarity that is in correspondence with the experimental data [4,6]. The branching ratios of the decay intensities of the one-step discrete $E1$ and $E2$ transitions are listed in Table I. The calculated results in Table I are compared with the available experimental data. Due to the small values of ratios $T[E1;I^+_{SD}\to(I-1)^-_{ND}]/T[E2;I^+_{SD}\to(I-2)^+_{SD}]$, the decay out through the one-step discrete transitions from the SD well to the ND well is strongly suppressed. We cannot explain the sharp decay out of the SD band by one-step $E1$ transitions. The one-step discrete γ rays to the ND states carry only a small fraction of the decay out of the SD states. After the decay out the spectrum has predominantly a statistical dipole character [3–6]. Let us consider below statistical transitions.

2. Statistical transitions

In order to determine Γ_{ND}, only statistical $E1$ transitions are considered for the decay between the ND states, since they are expected to dominate (with respect to the collective $E2$ and statistical $M1$ transitions [20,21]) due to the high excitation energy of the SD states above yrast line ($\approx$3–4 MeV). The latter comes from the fact that the moment of inertia for the SD shape is larger than the one for the ND states and the SD states become more excited with respect to the ND yrast line with decreasing spin I. The statistical $E1$ decay is governed by the level densities and the giant dipole resonance strength function based on the energy-weighted sum rule. The $E1$ width is approximated by the analytical expression $\Gamma_{ND}=3c_{E1}T^5$ [43], where $T=(U/a)^{1/2}$, an excitation energy $U=E(I)-\hbar^2I(I+1)/[2\mathcal{J}^r(|\eta|=1)]-2\Delta$ [44], a level density parameter $a=22.58$ MeV^{-1} [20,21,44], a backshift parameter $2\Delta=24/A^{1/2}$ and $c_{E1}=4!(e^2/\hbar c)\times(1/m_0c^2)(\Gamma_R/E_R)(NZ/A)$. The $E1$ giant resonance parameter are chosen as $E_R=78/A^{1/3}$ MeV and $\Gamma_R=4.4$ MeV [20,21].

The decay width $\Gamma_{SD}=\hbar B(E2)E^5_\gamma$ in the SD well is determined by collective rotational electromagnetic (nonstatistical) quadrupole transitions. The in-band $E2$ transition rate rapidly falls because of the growing fractional decrease in E_γ and E^5_γ dependence. The increase of Γ_{ND} with decreasing I is evident. In Figs. 17 and 18 the ratio Γ_{ND}/Γ_{SD} strongly grows as spin decreases. Near the band crossing point the statistical $E1$ decay to the ND configurations competes successfully with the collective $E2$ decay along the SD band.

The total probability P_{out} that the state in the SD well decays into the state in the ND well is calculated as follows:

$$P_{out}=\frac{c^2\Gamma_{ND}}{c^2\Gamma_{ND}+(1-c^2)\Gamma_{SD}}, \tag{9}$$

where c^2 is the fraction of wave function with the dominant SD component in the ND well. Here, the SD state has the partial width $(1-c^2)\Gamma_{SD}$ to decay in the next SD state and the partial width $c^2\Gamma_{ND}$ to decay in the lower-energy ND states.

One can see in Figs. 19 and 20 that the calculated total probabilities P_{out} are in good agreement with the experimental ones. This is an indication of validity of the cluster approach. The main reasons for the decay out near the band crossing point are: (1) the perceptible square of the amplitude of the SD wave function component in the ND well; (2) the reduction of the in-band SD collective $E2$ decay rate. The relative role of these two factors depends on the concrete nucleus (on the excitation energy of the SD state at the point of the decay out). The increase of P_{out} is mainly due to the increase of c^2 for the nuclei ^{190,192,194}Hg and ^{192,196}Pb, and

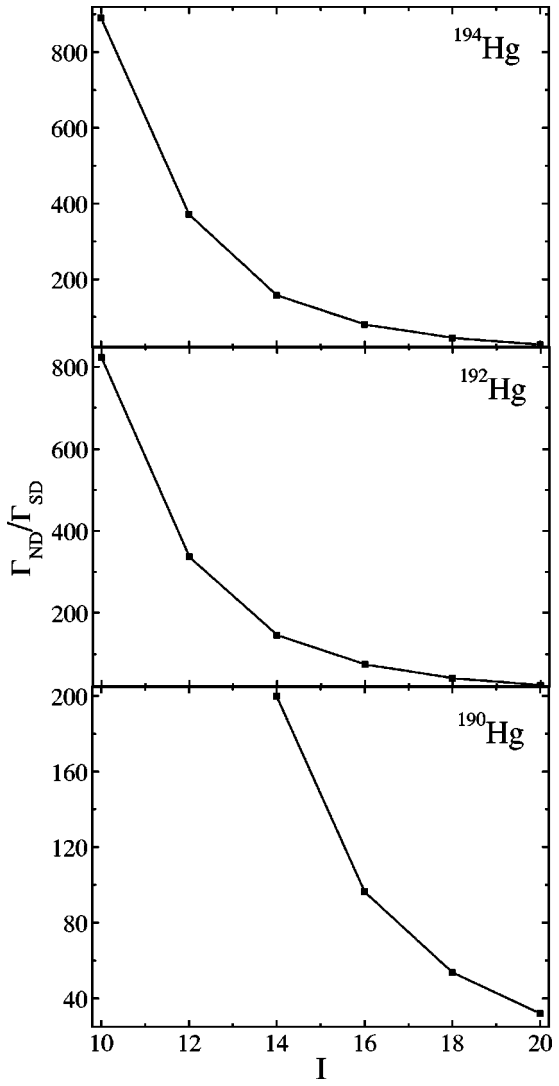

FIG. 17. The ratio (solid squares) between the decay width Γ_{ND} in the ND well and the decay width Γ_{SD} in the SD well as a function of spin I for nuclei ^{190,192,194}Hg. The solid line is to guide the eye.

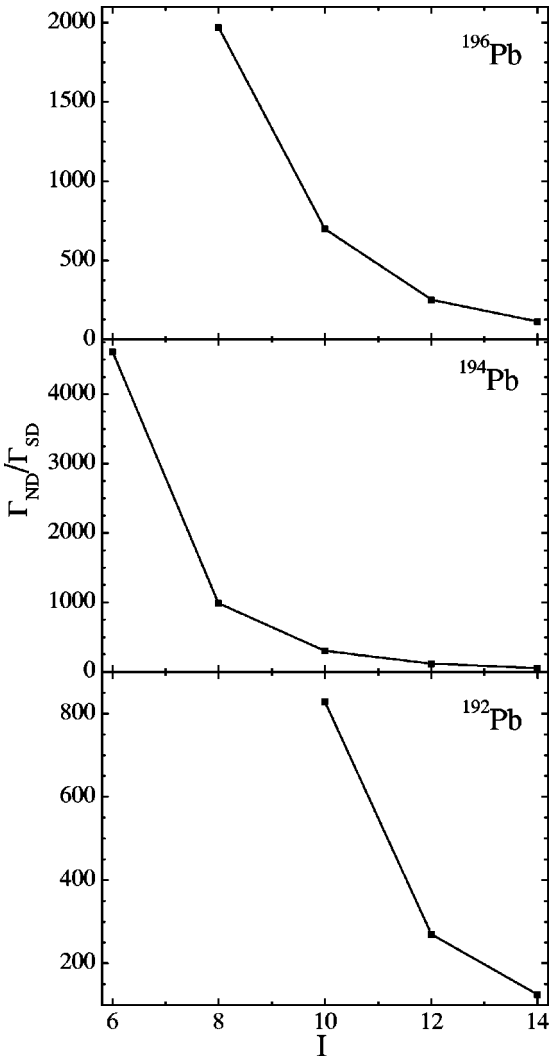

FIG. 18. The same as in Fig. 17, but for the isotopes of lead.

due to the decrease of Γ_{SD}/Γ_{ND} for ^{194}Pb where the excitation energy of the SD state at the decay out is the lowest ($I_{out}=6$) among the nuclei considered.

The origin of the decay out from the excited SD band is expected to be the same as for the decay out from the yrast SD band. The nature (α-cluster or two-quasiparticle-like structures) of the excited ND band which is crossed with the excited SD band is still unclear for us. Another open question is whether the mechanism underlying the transition from the ground and excited SD bands to the ND states in the mass regions with $A\approx 130$, 140, and 150 is the same as in the mass-190 region. With the cluster approach we reproduced recently the experimental data for the SD band of nucleus ^{60}Zn [36]. In this case the one-step discrete collective $E2$ γ rays to the ND yrast states explain the decay out of the SD band [2] since the width of collective $E2$ transitions in the ND well is much larger than the statistical one because of the small level density.

IV. SUMMARY

We conclude that the cluster approach provides a good description of the spectra and decay out of the lowest SD bands in the mass-190 region. The yrast SD band and ND band are related to ^{8}Be-cluster configuration (or two alphas on opposite sides of the heavy cluster) and to the α-particle clusterization, respectively. We postulated, as in many models in literature, that the decay out occurs through the ND doorway state. In our case the ND doorway state is the tail of the wave function of the zero-point vibration in the SD minimum which is calculated by solving the Schrödinger equation in charge asymmetry coordinate. At high excitation energy in the ND well, the ND doorway state is spread among the sea of dense compound states. This spreading leads to the large width of doorway state. So, the statistical mixing with highly excited ND states is one of the reasons for the decay out of the SD band. Our analysis indicates that the sudden decay out of the SD band takes place near the crossing of the SD band with the nearest neighboring excited ND band where the weight of the ND doorway state increases. Even at the near band crossing point the ND admixture c^2 in the SD

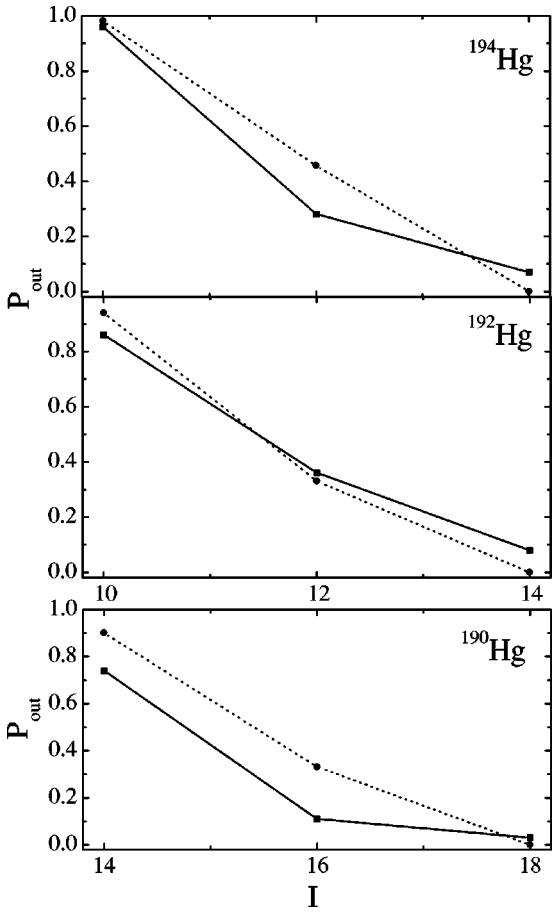

FIG. 19. The calculated (solid circles) probability P_{out} that the SD state decays into the ND states as a function of spin I for different isotopes of mercury. Experimental data (solid squares) are taken from Refs. [4,8,9]. The solid and dashed lines are to guide the eye.

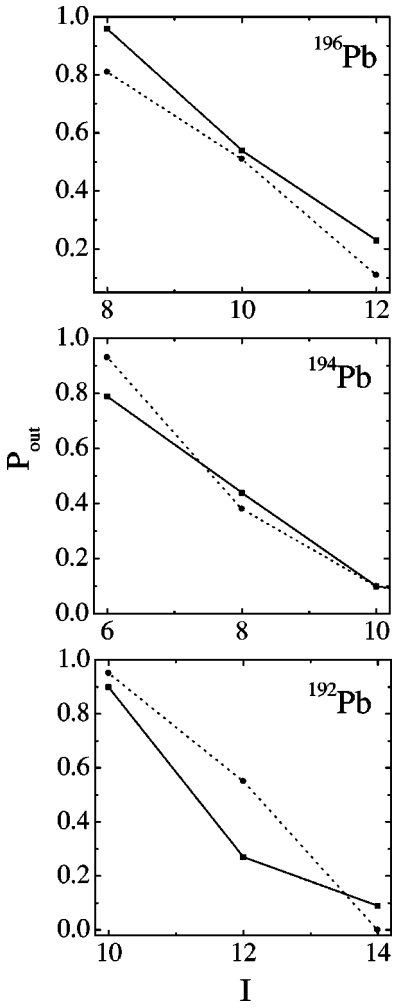

FIG. 20. The same as in Fig. 19, but for the isotopes of lead. Experimental data (solid squares) are taken from Refs. [6,5,10].

state is relatively small but the decay out occurs due to the large width of doorway state with respect to width of the SD state.

The maximal ND admixture of the SD states were found to be in the range of a few percent, thus revealing that the SD structure is essentially maintained down to the lowest observed SD states in the ground SD bands of the isotopes Hg and Pb. The SD minimum survives down to the SD bandhead.

A new method for the spectroscopic studies of the SD nuclei can be suggested within the cluster approach. During the γ emission the SD cluster states can decay into two clusters. Therefore, one can identify the SD states by measuring the rotational γ quanta in coincidence with the decay fragments of the DNS. If the SD state is a cluster state, we should observe relatively pronounced yields of the light clusters like α particles, ^{8}Be (two correlated α particles), and ^{12}C. This investigation of the SD states turns out to be not easy because of small penetrability of the Coulomb barrier for the clusters.

ACKNOWLEDGMENTS

We thank Dr. A. Dewald for fruitful discussions and suggestions. This work was supported in part by DFG (Bonn), Volkswagen-Stiftung (Hannover), and RFBR (Moscow).

[1] X.-L. Han and C.-L. Wu, At. Data Nucl. Data Tables **73**, 43 (1999); http://www.nndc.bnl.gov/nndc/ensdf/

[2] C. E. Svensson *et al.*, Phys. Rev. Lett. **82**, 3400 (1999).

[3] T. Lauritsen *et al.*, Phys. Rev. Lett. **89**, 282501 (2002); T. Lauritsen *et al.*, *ibid.* **88**, 042501 (2002).

[4] T. L. Khoo *et al.*, Phys. Rev. Lett. **76**, 1583 (1996); G. Hackman *et al.*, *ibid.* **79**, 4100 (1997).

[5] D. P. McNabb *et al.*, Phys. Rev. C **56**, 2474 (1997); A. N. Wilson *et al.*, Phys. Rev. Lett. **90**, 142501 (2003).

[6] A. Lopez-Martens *et al.*, Phys. Lett. B **380**, 18 (1996); J. R.

Hughes *et al.*, Phys. Rev. C **50**, R1265 (1994); K. Hauschild *et al.*, *ibid.* **55**, 2819 (1997).
[7] R. G. Henry *et al.*, Phys. Rev. Lett. **73**, 777 (1994); T. Lauritsen *et al.*, Phys. Rev. C **62**, 044316 (2000); A. Lopez-Martens *et al.*, Acta Phys. Pol. B **34**, 2195 (2003).
[8] A. N. Wilson *et al.*, Phys. Rev. C **54**, 559 (1996); B. Crowell *et al.*, *ibid.* **51**, R1599 (1995).
[9] P. Fallon *et al.*, Phys. Rev. C **51**, R1609 (1995); A. Korichi *et al.*, Phys. Lett. B **345**, 403 (1995); P. Willsau *et al.*, Nucl. Phys. **A574**, 560 (1994).
[10] D. Rossbach *et al.*, Phys. Rev. C **66**, 024316 (2002); D. Rossbach *et al.*, Phys. Lett. B **513**, 9 (2001); U. J. van Severen *et al.*, Z. Phys. A **353**, 15 (1995); S. Bouneau *et al.*, *ibid.* **358**, 179 (1997).
[11] I. Ragnarsson and S. Aberg, Phys. Lett. B **180**, 191 (1986); E. Vigezzi, R. A. Broglia, and T. Dossing, *ibid.* **249**, 163 (1990); Nucl. Phys. **A520**, 179 (1990); T. L. Khoo *et al.*, *ibid.* **A557**, 83 (1993).
[12] S. Aberg, Phys. Rev. Lett. **82**, 299 (1999); Nucl. Phys. **A649**, 392 (1999).
[13] C. A. Stafford and B. R. Barrett, Phys. Rev. C **60**, 051305 (1999); D. M. Cardamone, C. A. Stafford, and B. R. Barrett, Phys. Rev. Lett. **91**, 102502 (2003).
[14] J.-Z. Gu and H. A. Weidenmüller, Nucl. Phys. **A660**, 197 (1999).
[15] J. Libert, M. Girod, and J.-P. Delaroche, Phys. Rev. C **60**, 054301 (1999).
[16] R. Krücken, A. Dewald, P. von Brentano, and H. A. Weidenmüller, Phys. Rev. C **64**, 064316 (2001).
[17] Y. R. Shimizu, M. Matsuo, and K. Yoshida, Nucl. Phys. **A682**, 464c (2001); K. Yoshida, M. Matsuo, and Y. R. Shimizu, *ibid.* **A696**, 85 (2001).
[18] A. J. Sargeant *et al.*, Phys. Rev. C **65**, 024302 (2002); A. J. Sargeant *et al.*, *ibid.* **66**, 064301 (2002).
[19] A. Ya. Dzyublik and V. V. Utyuzh, Phys. Rev. C **68**, 024311 (2003).
[20] A. Dewald *et al.*, J. Phys. G **19**, L117 (1993); R. Krücken, A. Dewald, P. von Brentano, D. Bazzacco, and C. Rossi-Alvarez, Phys. Rev. C **54**, 1182 (1996); R. Kuhn *et al.*, *ibid.* **55**, R1002 (1997).
[21] R. Krücken *et al.*, Phys. Rev. C **55**, R1625 (1997); R. Krücken, *ibid.* **62**, 061302(R) (2000); A. Dewald *et al.*, *ibid.* **64**, 054309 (2001).
[22] P. Fallon *et al.*, Phys. Rev. Lett. **73**, 782 (1994).
[23] A. Korichi *et al.*, Phys. Rev. Lett. **86**, 2746 (2001).
[24] A. Prevost *et al.*, Eur. Phys. J. A **10**, 13 (2001).
[25] T. Nakatsukasa, K. Matsuyanagi, S. Mizotori, and Y. R. Shimizu, Phys. Rev. C **53**, 2213 (1996).
[26] D. Pansegrau *et al.*, Phys. Lett. B **484**, 1 (2000); D. Gassmann *et al.*, *ibid.* **497**, 181 (2001).
[27] P. G. Thirolf and D. Habs, Prog. Part. Nucl. Phys. **49**, 325 (2002).
[28] M. Freer and A. C. Merchant, J. Phys. G **23**, 261 (1997).
[29] H. Horiuchi and Y. K. Kanada-En'yo, Nucl. Phys. **A616**, 394 (1997).
[30] S. Cwiok *et al.*, Phys. Lett. B **322**, 304 (1994).
[31] S. Aberg and L.-O. Jonsson, Z. Phys. A **349**, 205 (1994).
[32] B. Buck, A. C. Merchant, and S. M. Perez, Phys. Rev. C **61**, 014310 (2000).
[33] T. M. Shneidman, G. G. Adamian, N. V. Antonenko, S. P. Ivanova, and W. Scheid, Nucl. Phys. **A671**, 119 (2000).
[34] T. M. Shneidman, G. G. Adamian, N. V. Antonenko, R. V. Jolos, and W. Scheid, Phys. Lett. B **526**, 322 (2002); Phys. Rev. C **67**, 014313 (2003).
[35] V. V. Pashkevich *et al.*, Nucl. Phys. **A624**, 140 (1997).
[36] G. G. Adamian, N. V. Antonenko, R. V. Jolos, Yu. V. Palchikov, and W. Scheid, Phys. Rev. C **67**, 054303 (2003).
[37] V. V. Volkov, Phys. Rep. **44**, 93 (1978); W. Greiner, J. Y. Park, and W. Scheid, *Nuclear Molecules* (World Scientific, Singapore, 1975).
[38] G. G. Adamian *et al.*, Int. J. Mod. Phys. E **5**, 191 (1996).
[39] P. Möller, J. R. Nix, W. D. Myers, and W. J. Swiatecki, At. Data Nucl. Data Tables **59**, 185 (1995).
[40] G. G. Adamian, N. V. Antonenko, and R. V. Jolos, Nucl. Phys. **A584**, 205 (1995).
[41] G. G. Adamian *et al.*, Acta Phys. Pol. B **34**, 2147 (2003).
[42] A. Bohr and B. R. Mottelson, *Nuclear Structure* (Benjamin, New York, 1975), Vol. II.
[43] T. Dossing and E. Vigezzi, Nucl. Phys. **A587**, 13 (1996).
[44] A. V. Ignatyuk, *Statistical Properties of Excited Atomic Nuclei* (Energoizdat, Moscow, 1983).